Optical amplification in the near-infrared in gas-filled hollow-core fibers

Daniele Faccio,[1,2,*] Alexander Grün,[1] Philip K. Bates,[1] Olivier Chalus,[1] and Jens Biegert[1,3]

[1]*ICFO-Institut de Ciènces Fotòniques, Mediterranean Technology Park, 08860 Castelldefels, Barcelona, Spain*
[2]*CNISM and Department of Physics and Mathematics, Università dell'Insubria, Via Valleggio 11, IT-22100 Como, Italy*
[3]*ICREA Institució Catalana de Recerca i Estudis Avançats, 08010 Barcelona, Spain*
**Corresponding author: daniele.faccio@uninsubria.it*

Received July 7, 2009; revised August 22, 2009; accepted August 24, 2009; posted August 27, 2009 (Doc. ID 113759); published September 18, 2009

We demonstrate efficient optical parametric amplification and generation in a gas-filled hollow-core fiber of near-infrared pulses, peaked at 1.4 μm wavelength, with 5 μJ energy and 45 fs duration at the fiber output. Numerical simulations confirm that the OPA is phase matched through excitation of higher-order fiber modes. © 2009 Optical Society of America

OCIS codes: 190.4380, 190.4975, 190.7110.

The development of few-cycle laser sources in the near-infrared (NIR) to mid-infrared (MIR) spectral region is attracting attention owing to applications in high-intensity laser-matter interactions [1]. However, a notable point, which should be considered, is the lack of available gain media with the required bandwidth to support lasing and generation of ultrashort (less than 50 fs) pulses in the NIR–MIR range. For this reason NIR–MIR ultrashort pulse generation schemes are, to date, all based on optical parametric amplification (OPA) in crystals with second-order, $\chi^{(2)}$, nonlinearity. For example, pulse energies up to 1 mJ and durations as short as 17 fs at a 1.4 μm wavelength have been reported using a 60 fs Ti:sapphire (Sa) laser as a pump source [2] and, more recently, a fiber-based pump scheme has been demonstrated with 100 kHz repetition rate at 3.4 μm wavelength [3,4]. A further advantage of the OPA process is that if the seed is generated and amplified by same pump laser the carrier-envelope phase (CEP) may be passively locked, thus providing a robust and alignment-free stabilization technique [5].

Recently, MIR generation mediated by the nonlinear Kerr effect was observed in ultrashort laser pulse filamentation pumped by a Ti:Sa laser source and seeded at the second-harmonic wavelength [6]. Efficient OPA has also been demonstrated in gas-filled hollow-core fibers with generation of UV light at the third-harmonic wavelength of the 800 nm Ti:Sa pump laser [7]. Gas-filled hollow-core fibers have become a paradigm in the generation of few-cycle pulses at the back-end of commercial Ti:Sa lasers [8] as they produce output pulses with excellent mode quality and a uniform temporal pulse profile across the transverse direction.

In this Letter, we present results that show for the first time, to our knowledge, OPA in a gas-filled hollow-core fiber with the generation of 1–2.5 μm NIR, 45 fs pulses with a peak wavelength at 1.4 μm and 5 μJ energy. Owing to the particular OPA scheme used we expect these pulses to have constant CEP. Phase matching of the OPA process is ensured by excitation of higher-order modes as also verified by numerical evaluation of the phase-matching relations.

The experimental layout is shown in Fig. 1. The pump pulse was generated by an amplified Ti:Sa laser and had 30 fs duration, 780 nm central wavelength. A weak nanojoule level second-harmonic seed pulse is created by frequency doubling the pump pulse in a 100-μm-thick beta-barium-borate (BBO) crystal tuned to the optimal phase matching angle (~30% conversion efficiency). The second harmonic is then strongly reduced by a dichroic mirror with high reflectivity at 400 nm. Roughly 1 nJ of the second-harmonic signal leaks through the mirror and copropagates with the pump pulse. The pump and seed pulses are focused with a 2 m focal length reflective mirror into a 1-m-long, hollow-core fiber with a 550 μm inner diameter filled with Ar at 1.4 bar. At ~1 m from the capillary input we placed an adjustable iris. Closing the iris increases the input pump beam diameter at the fiber input and also induces Fresnel diffraction rings: changing these features allows us to effectively change the coupling efficiency to the various modes of the hollow-core fiber. Finally the output was focused by an $f=30$ cm off-axis parabolic mirror and we then monitored either the spectrum (Ocean Optics spectrometers, HR4000 and NIR256–2.5), the spatial profile [InGaAs complementary metal-oxide semiconductor (CMOS) camera, Xenics,

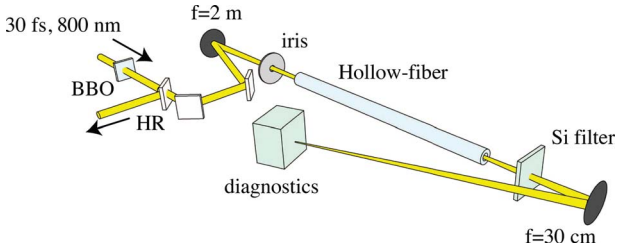

Fig. 1. (Color online) Experimental layout. The input Ti:Sa laser pulse (800 nm, 30 fs, 1.2 mJ) is duplicated in a 100-μm-thick BBO crystal. The fundamental and second-harmonic pulses are focused with an $f=2$ m focusing mirror into the hollow-core fiber (550 μm inner core diameter, 1 m length).

XEVA 202], or the temporal profile [with a home-built second-harmonic frequency-resolved optical gating (FROG)].

Figure 2 shows the measured spectra under conditions of optimal OPA and NIR pulse generation. The input 800 nm pulse spectrum, dashed curve in Fig. 2(b), is strongly reshaped and blueshifted toward 700 nm, solid curve in Fig. 2(b). The reason for this strong blueshift and bandwidth narrowing is most likely related to both a combination of self-phase modulation and plasma defocusing or absorption [9]. We also observed a similar spectral reshaping, albeit with a smaller shift to 750 nm, when removing the hollow-core fiber and freely focusing in air. The second-harmonic seed spectrum is shown Fig. 2(a). The dashed curve shows the input spectrum while the solid curve shows the amplified and broadened (by cross-phase modulation from the intense pump pulse) spectrum at the fiber output. Changing the iris diameter led to a rather dramatic change in the measured spectrum and output energy: both decreasing and increasing the aperture diameter gives a very strong reduction in the OPA efficiency and the spectrum quickly returns to be very similar to that measured at the input. An optimal aperture of 1.5 mm was found to give an amplified second-harmonic seed energy of 6 μJ with a gain factor of 6000.

Finally, Fig. 2(c) shows the NIR spectra. The solid curve shows the spectrum for the optimal conditions described above, corresponding to a total NIR energy of 5 μJ, measured after a 3.2-mm-thick silicon filter so as to block the pump and seed pulses. This energy was also optimized by changing the Ar gas pressure. Lower pressures led to a fast decrease in the OPA efficiency, whereas increasing the pressure above 1.4 bar led to similar, yet slowly decreasing, NIR energies. We note that we also tried to seed the OPA process with the full available second-harmonic energy, i.e., ~100 μJ, which was redirected into the hollow-core fiber after a delay stage and focused with a separate $f=2$ m focal length mirror. Even after careful optimization of the delay between the pump and seed pulses, the total NIR energy only increased to 6 μJ. This result would seem to imply that the OPA process is already close to saturation with the 1 nJ seed. Furthermore, we note that with the two-arm setup, a delay variation of less than 30 fs was sufficient to completely suppress all parametric effects. However, the simpler one-arm case shown in Fig. 1 did not require a delay stage in order to adjust the relative delay with the pump pulse, and the pulses were automatically synchronized inside the fiber. This is a rather surprising result, considering the fact that propagation in air after the focusing mirror should separate the pump and second-harmonic pulses by more than a pulse width. The reason for the spontaneous synchronization of the two pulses is still not fully clear but may be related to pulse lengthening due to chirp and possibly to dispersion effects in the dichroic mirror coating. The dashed curve in Fig. 2(c) corresponds to the spectrum calculated by taking all the possible four-wave-mixing combinations, $\omega_{\mathrm{NIR}}=\omega_i+\omega_j-\omega_k$, where ω_{NIR} is the NIR frequency and $\omega_{i,j,k}$ are frequencies taken within the pump and second-harmonic spectra as measured at the fiber output. As can be seen this calculation is able to reproduce both a relatively precise spectral peak wavelength and spectral shape. This supports the origin of the NIR pulse as due to OPA mediated by four-wave-mixing.

Figures 3(a) and 3(b) show the NIR pulse measured and retrieved spectrograms, respectively, obtained by second-harmonic FROG and Fig. 3(c) shows the retrieved the temporal intensity profile and the instantaneous frequency variation ($\Delta\omega$) (solid curves). The FWHM is found to be 82 fs. Accounting for the dispersion-induced pulse lengthening in the silicon filter, this corresponds to a 45 fs pulse at the hollow-core fiber output. The dashed curve is the Fourier transform of the total measured spectrum shown in Fig. 2(c) assuming a flat phase, indicating that the OPA process is capable of generating 10 fs FWHM pulses. Figure 3(d) shows the near-field intensity profile of the NIR pulse measured with an InGaAs CMOS camera. The pulse has a central peak

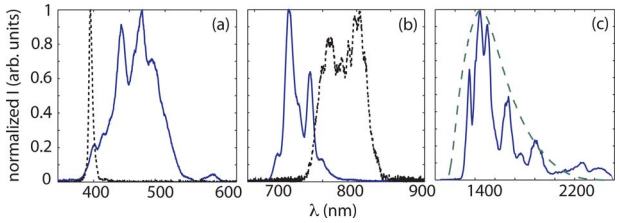

Fig. 2. (Color online) Measured spectra. (a) Dashed curve, input second-harmonic seed spectrum; solid curve, output amplified seed spectrum. (b) Dashed curve, input pump spectrum; solid curve, output pump spectrum. (c) Solid curve, NIR spectrum with 1 nJ seed; dashed curve, calculated NIR spectrum starting from the output spectra in (a) and (b).

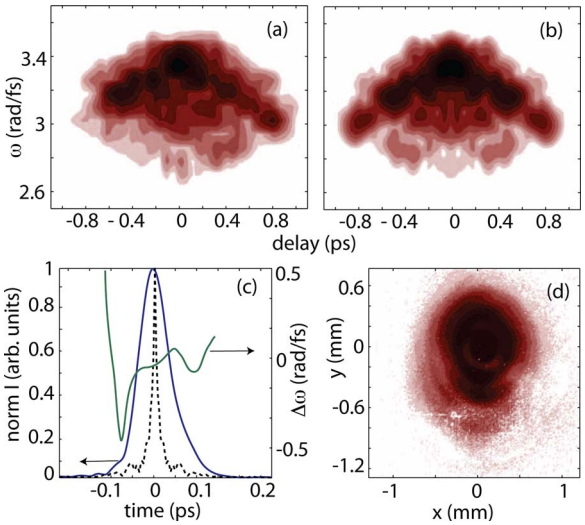

Fig. 3. (Color online) NIR temporal and spatial profiles. (a) and (b) are the measured and retrieved FROG spectrograms, respectively, in logarithmic scale (three decades). (c) Solid curves, retrieved temporal intensity and instantaneous frequency change ($\Delta\omega$) with a FWHM of 82 fs (FROG error 0.8%); dashed curve, Fourier transform of the spectrum in Fig. 2(c) with a FWHM of 10 fs. (d) is the spatial near-field profile of the NIR pulse, in logarithmic scale (three decades).

surrounded by a weaker ring, indicating that most of the NIR energy is concentrated in the fiber second-order mode. This higher mode is due to the fact that four-wave mixing is not phase matched if all the pulses are in the fiber lowest-order mode. On the contrary it is possible to find phase-matching conditions that give efficient OPA by exciting (with an appropriate input iris aperture) higher-order modes.

We verify this assertion by analytically estimating the optimal phase-matching conditions inside the fiber, i.e., by evaluating the four-wave-mixing coherence length $\ell_c = \pi/|\Delta\beta|$. The phase mismatch $|\Delta\beta|$ is a function of gas pressure (P), interacting wavelengths (λ), and hollow-core fiber radius (a),

$$\Delta\beta = 2\beta_{\text{pump}} - \beta_{\text{seed}} - \beta_{\text{NIR}}. \tag{1}$$

The fiber-mode wave vector is [10]

$$\beta = \frac{2\pi n(\lambda,P)}{\lambda}\left\{1 - \frac{1}{2}\left[\frac{u_{m,n}\lambda n(\lambda,P)}{2\pi a}\right]^2\right\}, \tag{2}$$

where $u_{m,n}$ is the nth root of the mth Bessel function, $J_m(u_{m,n})=0$, and $n(\lambda,P)$ is the pressure-dependent refractive index of argon [11]. Figure 4(a) shows the coherence length for a fixed capillary radius $a = 225\ \mu$m and varying gas pressure for three different mode combinations (p,q,r) where p, q, and r are the mode orders of the fundamental, seed, and NIR signal, respectively. These curves allow us to predict efficient phase matching (i.e., the coherence length is longer than the fiber length) for wavelengths at ~1.3, ~1.4, and ~1.7 μm, in close agreement with the peaks in the experimentally measured spectrum [see Fig. 2(c)]. The important feature here is that the phase matching is ensured through the interaction of higher order modes. As a further confirmation of multimodal propagation and interaction within the fiber we measured the NIR spatial far-field profile, Fig. 4(b). This shows a clear ring-type shape in keeping with a Bessel-like higher order fiber mode.

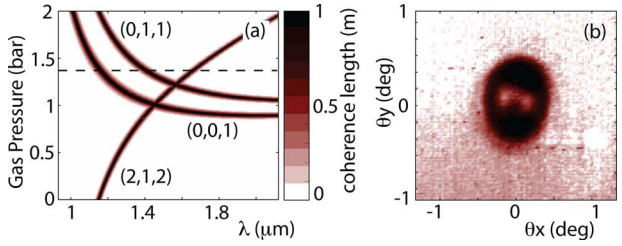

Fig. 4. (Color online) (a) Analytically evaluated coherence length for varying argon gas pressure. The three shaded areas show the coherence length for different combinations (p,q,r) where p, q, and r, are the mode orders of the fundamental, seed and NIR signal, respectively. The dashed curves gives the intersection at the experimentally optimized pressure of 1.4 bar, indicating expected NIR maxima at ~1.3, ~1.4, and ~1.7 μm. (b) The measured far-field distribution of the NIR mode.

In conclusion we have demonstrated efficient OPA in an Ar-filled hollow-core fiber and generation of ultrashort NIR pulses in a setup that is extremely simple. The NIR pulses may either be used directly for nonlinear laser pulse–matter interactions or they may be used as a high-energy seed for improved contrast in $\chi^{(2)}$ parametric amplification schemes. Finally we note that the four-wave-mixing process involved in the OPA is expected to lead to CEP stable pulses [6], a further feature of great importance for applications in extreme nonlinear optics.

D. Faccio acknowledges support from Marie Curie grant, contract PIEF-GA-2008-220085. J. Biegert acknowledges support from the Spanish Ministry of Education and Science through its Consolider Program Science (grant SAUUL—CSD 2007-00013) as well as through Plan Nacional (grant FIS2008-06368-C02-01).

References

1. P. Colosimo, G. Doumy, C. I. Blaga, J. Wheeler, C. Hauri, F. Catoire, J. Tate, R. Chirla, A. M. March, G. G. Paulus, H. G. Muller, P. Agostini, and L. F. DiMauro, Nat. Phys. **4**, 386 (2008).
2. C. Vozzi, F. Calegari, E. Benedetti, S. Gasilov, G. Sansone, G. Cerullo, M. Nisoli, S. De Silvestri, and S. Stagira, Opt. Lett. **32**, 2957 (2007).
3. C. Erny and K. Moutzouris, Opt. Lett. **32**, 1138 (2007).
4. O. Chalus, P. K. Bates, M. Smolarski, and J. Biegert, Opt. Express **17**, 3587 (2009).
5. A. Baltuška, T. Fuji, and T. Kobayashi, Phys. Rev. Lett. **88**, 133901 (2002).
6. T. Fuji and T. Suzuki, Opt. Lett. **32**, 3330 (2007).
7. C. G. Durfee III, S. Backus, M. M. Murnane, and H. C. Kapteyn, Opt. Lett. **22**, 1565 (1997).
8. M. Nisoli, S. De Silvestri, O. Svelto, R. Szipöcs, K. Ferencz, Ch. Spielmann, S. Sartania, and F. Krausz, Opt. Lett. **22**, 522 (1997).
9. J. K. Koga, J. Opt. Soc. Am. B **26**, 930 (2009).
10. E. A. J. Marcatili and R. A. Schmeltzer, Bell Syst. Tech. J. **43**, 1783 (1964).
11. A. Dalgarno and A. E. Kingston, Proc. R. Soc. London, Ser. A **259**, 424 (1960).